

Evaluation of cosmogenic Ge-68 background in a high purity germanium detector via a time series fitting method

W.H. Dai^a, J.K. Chen^a, H. Ma^{a,*}, Z. Zeng^a, M.K. Jin^a, Q.L. Zhang^a, J.P. Cheng^{a,b}

^aKey Laboratory of Particle and Radiation Imaging (Ministry of Education) and Department of Engineering Physics, Tsinghua University, Beijing 100084

^bCollege of Nuclear Science and Technology, Beijing Normal University, Beijing 100875, China

Abstract

Ge-68 is a cosmogenic isotope in germanium with a half-life of 270.9 days. Ge-68 and its decay daughter Ga-68 contribute considerable background with energy up to 3 MeV to low background γ spectrometers using high purity germanium (HPGe) detectors. In this paper, we evaluated the background of Ge-68 and Ga-68 in a *p*-type coaxial HPGe detector operated at China Jinping underground laboratory (CJPL) via a time series fitting method. Under the assumption that Ge-68 and Ga-68 are in radioactive equilibrium and airborne radon daughters are uniformly distributed in the measurement chamber of the spectrometer, we fit the time series of count rate in 1-3 MeV to calculate the Ge-68 activity, radon daughter concentrations, and the time-invariant background component. Total 90 days measured data were used in analysis, a hypothesis test confirmed a significant Ge-68 signal at 99.64% confidence level. The initial activity of Ge-68 is fitted to be $477.0 \pm 112.4 \mu\text{Bq/kg}$, corresponding to an integral count rate of 55.9 count/day in 1-3 MeV range. During the measurement, Ge-68 activity decreased by about 30%, contributing about 62% of the total background in 1-3 MeV range. Our method also provides an estimation of the variation of airborne radon daughter concentrations in the measurement chamber, which could be used to monitor the performance of radon reduction measures.

Keywords: high purity germanium detector, cosmogenic Ge-68, time series analysis

*Corresponding author: mahao@tsinghua.edu.cn

1. Introduction

High purity germanium (HPGe) detectors have been widely used in radiation monitoring, nuclear physics, particle physics, and astrophysics due to its high energy resolution, high stopping power and low intrinsic background [1, 2, 3]. The use of HPGe detector as γ spectrometer requires strict control and accurate measurement of background for detecting trace radioactivity within the sample. For γ spectrometers operated at underground laboratories, the rock overburden reduces the cosmic-ray muon flux by several orders of magnitudes, for instance, 1000 m rock can reduce cosmic-ray muon flux by over 10^5 times [4]. External γ can be shielded by high-Z materials like copper and lead, neutron can be shielded by borated polyethylene. However, the cosmogenic radioactive isotopes cumulated during the fabrication and transportation of detector above ground can continuously contribute background after the detector have been moved underground. As the production of cosmogenic isotopes becomes negligible underground [5], their activities decrease after detector arrived underground, leading to a change of background in the measured spectrum. Therefore, a measurement of their initial activity and an evaluation of their background during detector's underground operation are important for the understanding and modeling of the background.

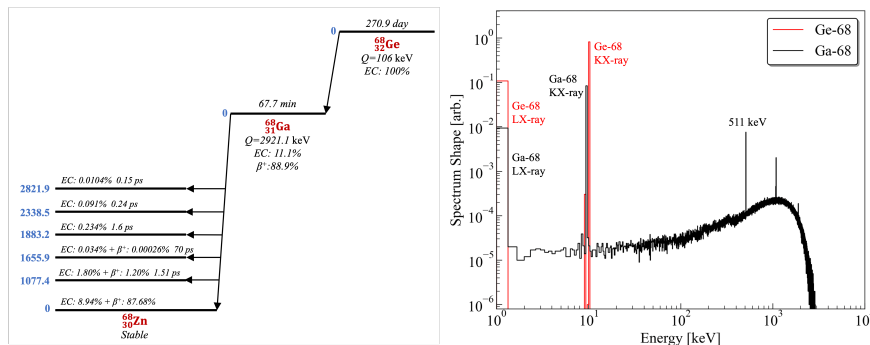


Figure 1: Left panel: decay scheme of Ge-68 and Ga-68, data from[6]. Right panel: typical Ge-68 and Ga-68 spectra in a HPGe detector, the spectra are simulated via Geant4[7, 8, 9] using a 1-kg cylinder Ge model with 0.5 mm deadlayer at the surface (energy resolution not considered).

Ge-68 is a cosmogenic isotope produced by nuclear reactions between germanium nucleus and high energy cosmic-rays (neutron, proton, and γ). At sea level, the production rate is around $80\text{-}120 \text{ kg}^{-1}\text{day}^{-1}$ for different latitudes and longitudes [10], corresponding to a saturated activity of $0.93\text{-}1.39 \text{ mBq/kg}$. Ge-68 decays to Ga-68 via electron capture (EC) with a half-life of 270.9 days (decay scheme in Fig.1) [6]. Its decay emits X-rays and auger electrons with total energy equals to the binding energy of the captured electron ($<11 \text{ keV}$), therefore only contributes background at low energy region (as in Fig.1(right)). Ga-68 decays to Zn-68 with a Q -value of 2921.1 keV and a half-life of 67.7 min

[6], its decay scheme is shown in Fig.1(left). In most case, Ga-68 decays to ground state of Zn-68 via β^+ mode and emit a positron with maximum kinetic energy up to 1899.1 keV. The spectrum shape of Ga-68 in HPGe detector is shown in Fig.1(right), it manifests a arc-shaped line with a small peak from 511 keV annihilation photons and summed peaks around 1 MeV from γ and X-rays in EC decay mode. Due to the relative short half-life of Ga-68, it will be in radioactive equilibrium with Ge-68. Ga-68 with activity of 1 mBq/kg could contribute a background of approximate 85 count/day/kg_{Ge} at 60-2700 keV range, which is comparable to the typical background level of an underground HPGe γ -spectrometer [11].

There are general two ways of measuring the Ge-68 activity, one is analyzing the 10.38 keV KX-ray peak in the spectrum [10, 12, 13]. However, this method is not feasible for detectors with dynamical range cannot cover the low energy range. The other way is fitting the count rate at different time. Once the detector arrives underground, the decay of Ge-68 and Ga-68 will lead to a decrease of count rate in the spectrum. Fitting the count rate with Ge-68 half-life could provide an estimation of the activity, but requires decoupling other time variant components, e.g., count rate change caused by concentration variation of the airborne radon daughter. We develop a method fitting the count rate with Ge-68 decay component and the variation of radon daughter simultaneously while constraining the radon daughter concentration by its characteristic peaks. This method is then applied to measuring the activity of Ge-68 in a HPGe detector operated in China Jinping underground laboratory (CJPL)[14].

This paper is organized as follows: Sec.1 gives the background of this work. Sec.2.1 introduces the detector, fitting method and statistic test method. Sec.3 provides the fitting results and interpretation of the results. Sec.4 summaries the this work and outlooks the possible applications of our method.

2. Method

2.1. HPGe detector at CJPL

The HPGe detector studied is a low background *p*-type coaxial HPGe detector purchase from CANBERRA, and is used as the detector of a low background γ -spectrometer at CJPL. It has a Ge crystal of 2.48 kg with 0.5 mm deadlayer and a energy threshold of 100 keV, the crystal and its surrounding structure are shown in the left panel of Fig.2 [15]. After the detector been manufactured in France, it was shipped to CJPL via truck and train, it arrived at CJPL at 2020/07/25 with approximate 1 month exposure time above ground [15].

After arrived at CJPL, the detector is shielded by copper and lead to reduce the background from environmental γ -rays. The shielding is made of 10 cm underground storage copper and 20 cm lead (5 cm ancient Poland lead and 15 cm modern lead), the structure of the Cu/Pb shielding is illustrated at Fig.2. Nitrogen gas has been constantly injected into the detector chamber inside copper shielding to reduce the radon concentration.

The energy calibration was performed using Co-60, Co-57, and Eu-152 sources[15]. After the calibration, the sources are removed and detector was operated to

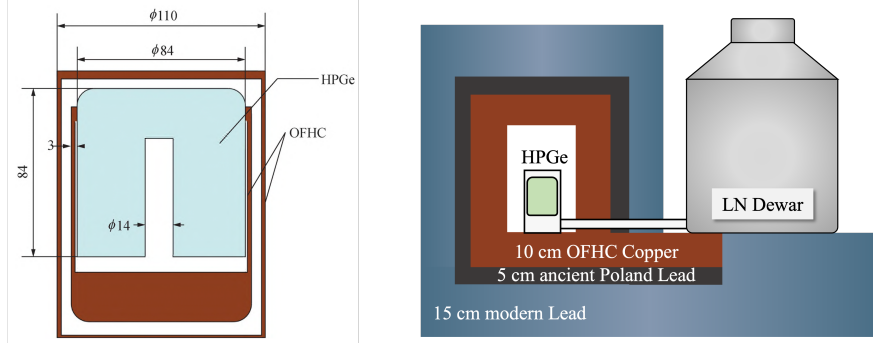


Figure 2: Left panel: structure of the HPGe detector. Right panel: structure of the detector's shielding, the shielding consists of innermost 10 cm OFHC copper, 5 cm ancient Poland lead, and outmost 15 cm modern lead.

measure the background. The spectrum was saved regularly, each saved spectrum corresponds to 6 hours live measurement time. Total 90 days background measurement data is cumulated and used to calculate the activities of cosmogenic isotopes. The measurement of Mn-54, Co-57, and Co-58 activities via fitting their characteristic peaks could be found in[15]., this work focus on the measurement of Ge-68 activity.

2.2. Time series fitting method

The calculation of Ge-68 activity via fitting the variation of count rate requires decoupling various time variant and invariant background. The time-variant background considered are cosmogenic isotopes with relative short half-life and radon daughters in the void volume between the detector and copper shield. The time invariant background are those from radioisotopes with long half-life, for instance, γ -rays from U, Th decay chain and K-40. And for background from Co-60, as the half-life of Co-60 (1925.3 day) is much longer than the measure time (90 days), its activity decreases only 3% during the measurement, therefore, it is treated as a time invariant background in this work. The count rate in a specified energy range can be modeled as eq.1

$$R_i(t, t + \Delta t) = \sum_k^{N_{Iso}} \frac{A_{0,k}}{\Delta t} \cdot \frac{T_{1/2,k}}{\ln 2} \cdot e^{-\frac{\ln 2}{T_{1/2,k}} t} [1 - e^{-\frac{\ln 2}{T_{1/2,k}} \Delta t}] \cdot \varepsilon_{k,i} \quad (1)$$

$$+ \sum_p^{N_{Rn}} C_p(t) \cdot \varepsilon_{p,i} + B_i,$$

the specified energy range is indicated by i , $R_i(t, t + \Delta t)$ is the count rate in i energy range at $t \sim t + \Delta t$ interval. The first item in eq.1 is the sum of contribution from each cosmogenic isotope k , $A_{0,k}$ is the initial specific activity at $t = 0$ (units: Bq/kg), and $T_{1/2,k}$ is the decay half-life. $\varepsilon_{k,i}$ is the detection efficiency

of the decay products of k isotope in i energy range (units: cpd/(Bq/kg), cpd as count per day). N_{Iso} is the total number of cosmogenic isotopes. The second item $\sum_p C_{p,i} \cdot \varepsilon_{p,i}$ is the sum of contribution from radon daughters. In this work, we treat each radon daughter independently as they are not in equilibrium, but make the assumption that they are uniformly distributed in the void volume inside copper shield. $C_p(t)$ is the average concentration of radon daughter p (units: Bq/m³) in $t \sim t + \Delta t$ interval. $\varepsilon_{p,i}$ is the detection efficiency of γ -rays emitted by p isotope in i energy range (units: cpd/(Bq/m³)). N_{Rn} is the total number of considered radon daughter. B_i is the time-invariant component in i energy range (units: cpd).

We built the detector and its shielding structure in Geant4[7, 8, 9] to simulate the detection efficiency of different background sources. The simulation is performed using Geant4 version 11.0.3 with the *shielding* physics list. In simulation, the energy deposition in the surface deadlayer is not recorded, and the energy resolution of the detector is considered using the calibrated energy resolution function: $FWHM/\text{keV} = 0.9903 + 0.3197\sqrt{E/\text{keV}} + 5.789 \times 10^{-5} \times (E/\text{keV})^2$ [16]. The efficiencies $\varepsilon_{k,i}$ and $\varepsilon_{p,i}$ are then calculated by:

$$\varepsilon_{k,i} = \frac{n_i}{N_S} \cdot m_{Ge}, \quad (2)$$

$$\varepsilon_{p,i} = \frac{n_i}{N_S} \cdot V_{Chamber}, \quad (3)$$

where N_S is the total number of simulated particles, n_i is the observed count in i energy range in simulated spectrum, $m_{Ge}=2.48$ kg is the mass of Ge crystal, $V_{Chamber}=9.4$ dm³ is the volume of the detector chamber inside copper shielding.

The activity of cosmogenic isotope ($A_{0,k}$) and radon daughter concentration ($C_p(t)$) can be calculated via fitting the modeled count rate to measured data using a maximum likelihood method. The observed count in each time interval obeys Poisson distribution, therefore the likelihood function can be written as:

$$\mathcal{L} = \prod_i^{N_E} \prod_t^{N_T} \frac{\lambda_{i,t}^{n_{i,t}}}{n_{i,t}!} e^{-\lambda_{i,t}}, \quad (4)$$

$$\lambda_{i,t} = R_i(t, t + \Delta t) \cdot \Delta t, \quad (5)$$

where $\lambda_{i,t}$ and $n_{i,t}$ is the expected and observed count in i energy range at $t \sim t + \Delta t$ interval. N_E is the number of selected energy interval and N_T is the number of time interval. The total number of fitting parameters is $N_{Iso} + N_{Rn} \cdot N_T + N_E$, corresponding to number of cosmogenic isotopes, radon daughter concentration, and time-invariant background. And the number of observed data is $N_E \cdot N_T$ corresponding to the count rate series in each energy range. To better constrain the fitting parameters, multiple energy ranges are required, they should at least include the signal of cosmogenic isotopes and characteristic peak of radon daughter. It should be noted that the fitted of radon daughter

concentration $C_p(t)$ is only sensitive to the variation of its concentration, the constant part will be regarded as a time-invariant background.

In the calculation of Ge-68 activity, we select three energy ranges: 609 ± 5 keV, 1764 ± 6 keV, and $1000\sim 3000$ keV, the first two are characteristic peaks of radon daughter Bi-214, and the third is chosen as the signal region of Ge-68 and its decay daughter Ga-68. We assume the Ge-68 and Ga-68 are in equilibrium, and hereafter use Ge-68 to indicate Ge-68 and Ga-68. We only consider two time variant components: Ge-68 and radon daughter Bi-214. Using activities determined in our previous work[15], other cosmogenic isotopes (Mn-54, Co-57, and Co-58) contributes negligible background in the selected energy regions (less than 1%), therefore are omitted in this work. The total 358 spectra measured in 6 hours interval are merged into 30 spectra, each corresponds to 3 days live measurement time. The count rate in each energy range is calculate for the 30 spectra, and total 90 count rate data are used for analysis.

The fitting of the parameters is by maximum the likelihood function \mathcal{L} in eq.4. We use the Markov Chain Monte Carlo (MCMC) method[20] to calculate the best fit result and the corresponding uncertainty. The calculation is performed using the *UltraNest* MCMC toolkit[17] in *python3* platform.

2.3. Statistic test of the significance of Ge-68 signal

In order to evaluate the significance of Ge-68 signal, we perform a hypothesis test: the null hypothesis (H_0) is that there are no Ge-68 in the measured data, and the alternative hypothesis (H_1) is the best fit result. For the null hypothesis, Bi-214 concentration and time-invariant background are fitted using the same procedure while setting the Ge-68 activity to 0.

The P value is used to test the coincidence between the hypothesis and measurement. It is defined as the probability of getting a worse result than observed in the measurement under a specified hypothesis[18]. In this work, it is calculated by:

$$P(H_i) = \int_{-\infty}^{s_{obs}(H_i)} f(s|H_i) dt \quad (i = 0, 1), \quad (6)$$

$$s(H_i) = \sum_t^{N_T} n_t \cdot \lambda_t(H_i) - \lambda_t(H_i) - \ln(n_t!), \quad (7)$$

where $s(H_i)$ is the test statistic defined as the sum of likelihood value in the 1-3 MeV Ge-68 signal region. $\lambda_t(H_i)$ is the expected count in $t \sim t + \Delta t$ interval under H_i hypothesis. $s_{obs}(H_i)$ is the observed value of $s(H_i)$, and is calculated via eq.7 using measured data. $f(s|H_i)$ is the probability distribution function (PDF) of test statistic s under H_i hypothesis.

$f(s|H_i)$ is calculated via a toy Monte Carlo method: n_t are randomly sample by Possion distribution using $\lambda_t(H_i)$ as the expectation. $s(H_i)$ is then calculated and stored for a group of sampled n_t ($t = 1, 2, \dots, N_T$) as a hypothesis

experiment. Then the hypothesis experiment is performed for 20,000 times to get the PDF of $s(H_i)$.

The P value of the alternative hypothesis ($P(H_1)$) demonstrates the goodness of the fit, while the P value of the null hypothesis ($P(H_0)$) indicates if adding Ge-68 in fitting is necessary. The significance of Ge-68 signal is the combination of a small $P(H_0)$ and a large $P(H_1)$.

2.4. Evaluation of the minimum detection activity

The minimum detection activity (MDA) of a γ spectrometer relies on the background level, the measured time, the analyzed characteristic peak, and the detection efficiency. If other factors are kept constant, the decay of Ge-68 will lead to a decrease of background and an improvement of the MDA.

Here we consider a typical "pair measurement" to evaluate the improvement of MDA by the decrease of Ge-68 background. In a pair measurement, the sample and background are measured for the same time (t_m), and the MDA is written as[19]:

$$MDA = \frac{2.71 + 4.65\sqrt{b_i(t_U, t_m)}}{\varepsilon \cdot I_\gamma \cdot t_m}, \quad (8)$$

where i indicates the selected characteristic peak, t_U is the underground operation time before the sample measurement, I_γ is the yield of the characteristic γ line, ε is the detection efficiency, $b_i(t_U, t_m)$ is the background count in the analysis window ($E_i \pm 3\sigma_{E_i}$), E_i is the energy of the characteristic γ line σ_{E_i} is the energy resolution. Background $b_i(t_U, t_m)$ is calculated using the 90 days background spectrum and the fitted Ge-68 activity ($A_{0, \text{Ge-68}}$) via:

$$b_i(t_U, t_m) = R_{i, \text{others}} \cdot t_m + A_{0, \text{Ge-68}} \cdot \frac{T_{1/2}}{\ln 2} \cdot e^{-\frac{\ln 2}{T_{1/2}} t_U} [1 - e^{-\frac{\ln 2}{T_{1/2}} t_m}] \cdot \varepsilon_{\text{Ge-68}, i}, \quad (9)$$

where $R_{i, \text{others}}$ is the measured background rate in i characteristic peak region subtracting the background from Ge-68 using eq.1. $\varepsilon_{\text{Ge-68}, i}$ and $T_{1/2}$ are the detection efficiency and half-life of Ge-68.

Here we set measure time t_m to 30 days, and the improvement of MDA after underground operation time (t_U) can be written as the ratio of MDA between t_U and $t_U = 0$:

$$\frac{MDA(t_U)}{MDA(t_U = 0)} = \frac{2.71 + 4.65\sqrt{b(t_U, t_m)}}{2.71 + 4.65\sqrt{b(t_U = 0, t_m)}} \quad (10)$$

3. Result and discussion

3.1. Detection efficiency of Ge-68 and radon daughter Bi-214

Total 10^7 and 10^8 particles are simulated for calculating the detection efficiencies of Ge-68 and airborne Bi-214, the simulated spectra are shown in Fig.3. For airborne Bi-214, its detection efficiencies in 609 ± 5 keV, 1764 ± 6 keV, and $1000\sim 3000$ keV energy ranges are 3.1, 0.73, and 7.6 cpd/(Bq/m³), respectively. For Ge-68, the efficiencies are 0.71, 1.20, and 132.3 cpd/(mBq/kg), respectively.

The count rate from 1 mBq/kg Ge-68 is equal to that from 17.4 Bq/m³ airborne Bi-214 in 1-3 MeV energy region. And the saturated activity of Ge-68 at sea level is around 1 mBq/kg[10]. This indicates that despite the spectrum of Ge-68 has no significant characteristic peak, it still can contribute a significant background in the total spectrum.

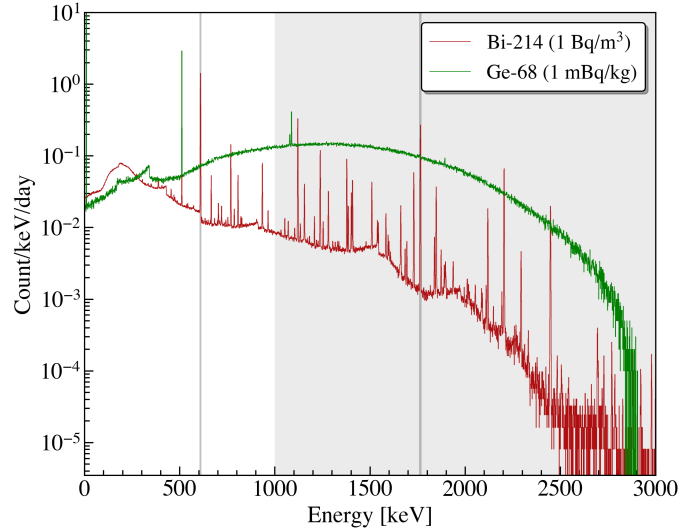


Figure 3: The simulated spectra of 1 mBq/kg Ge-68 and 1 Bq/m³ radon daughter Bi-214. The Ge-68 spectrum includes contribution from its decay daughter Ga-68 under equilibrium assumption. The three selected energy windows are labeled in gray.

3.2. Fitting result of Ge-68 activity

The count rates in 609 ± 5 keV, 1764 ± 6 keV, and $1000\sim 3000$ keV energy ranges of the 30 measured spectra are fitted with contribution from Ge-68, radon daughter Bi-214, and time-invariant background. The fit results are shown in Fig.4, and are in good agreement with the measured data. The residuals between fitted and measured data are around 0 and mostly within the 3σ band of the statistical uncertainties in measured data. Our method decoupling the contribution from Ge-68 and radon daughter Bi-214 as in Fig.4, the 609 ± 5 keV and 1764 ± 6 keV region are dominated by the contribution of Bi-214 and provide

a strong constraint to the Bi-214 concentration during the measurement. In the 1-3 MeV region, the contribution from Bi-214 is about 9.4% of the total count rate, Ge-68 contributes about 62.0% of the total count rate and is the most dominated background source.

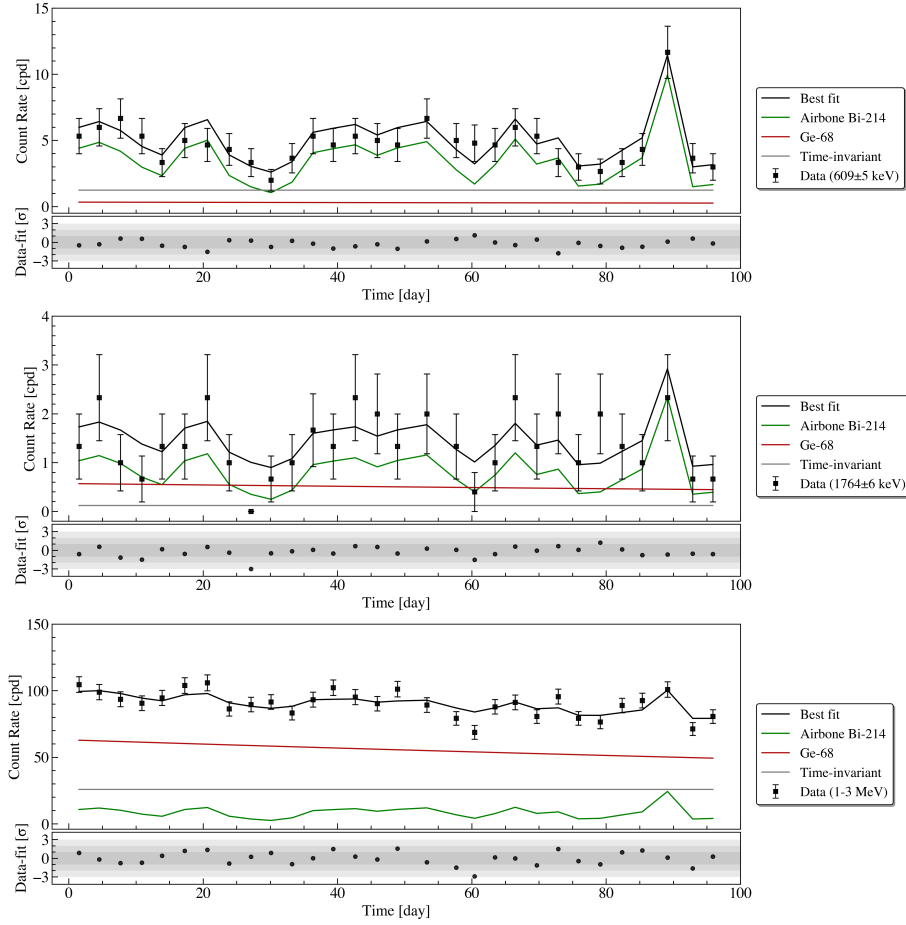


Figure 4: The best fit result of count rate in 609 ± 5 keV, 1764 ± 6 keV, and $1000\sim 3000$ keV. The best fit curves are labeled in black, the fitted contributions from Ge-68, Bi-214, and time-invariant background are labeled in red, green, and gray respectively. The residuals between the best fit and measured data are shown below the best fit curves.

The significance of Ge-68 signal is tested using method described in Sec.2.3. The calculated PDF of the test statistic $f(s)$ for null and alternative hypothesis are shown in Fig.5 along with the observed value (s_{obs}). The P value of the null hypothesis $P(H_0)=0.036\%$, which excludes the no Ge-68 hypothesis at 99.64% confidence level. The P value of the alternative hypothesis $P(H_1)=33\%$, demonstrates the goodness of the fit and indicates a significant Ge-68 signal in the measured data.

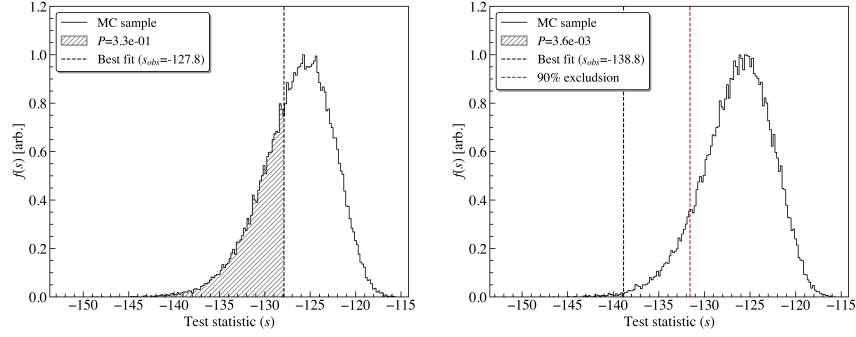


Figure 5: The significance test of Ge-68 signal. The left panel is the PDF of test statistic s under alternative hypothesis (the best fit result in Fig.4), The right panel is the PDF of s under null hypothesis (no Ge-68 signal).

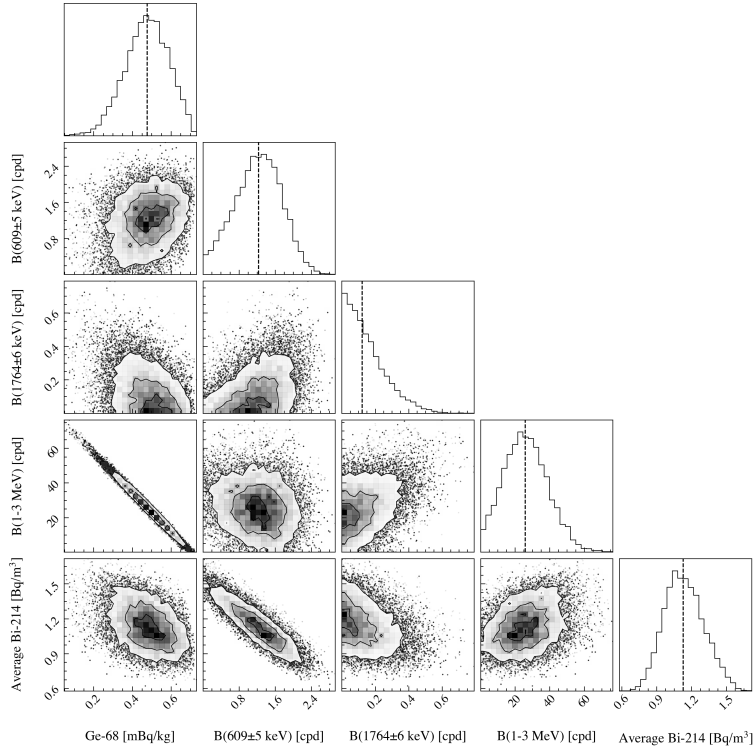


Figure 6: Contours for pairs of parameters in the *UltraNest* MCMC sampling, and the projected likelihood distribution for each parameter. The colors indicates the relative value of the likelihood distribution, each vertical dash lines indicates the median position. For simplicity, the Bi-214 concentrations at different times are combined to an average value.

Table 1: Fit results of Ge-68 initial activity ($A_{0,\text{Ge-68}}$), time-invariant background (B), and Bi-214 concentration ($C_{\text{Bi-214}}$). For simplicity, the Bi-214 concentrations at different times are combined to an average value.

Parameter	Units	Value	Note
$A_{0,\text{Ge-68}}$	$\mu\text{Bq/kg}$	476.95 ± 112.38	Ge-68 initial activity
$B_{609 \pm 5 \text{ keV}}$	cpd	1.24 ± 0.53	time-invariant background
$B_{1764 \pm 6 \text{ keV}}$	cpd	0.12 ± 0.12	time-invariant background
$B_{1 \sim 3 \text{ MeV}}$	cpd	25.81 ± 12.71	time-invariant background
$C_{\text{Bi-214}}$	Bq/m^3	1.42 ± 0.17	average Bi-214 concentration

The fitted Ge-68 initial activity is $477.0 \pm 112.4 \mu\text{Bq/kg}$, the uncertainty corresponding to the 68% confidence interval in the likelihood distribution derived from the *UltraNest* MCMC sampling. Values and uncertainties of other parameters are listed in Tabel.1. Fig.6 demonstrates the contours for pairs of parameters in the MCMC sampling, which shows the correlation between each pairs of parameters. The largest correlation is between Ge-68 activity and time-invariant background in 1-3 MeV, which is also the main contributor of the uncertainty of Ge-68 activity.

3.3. Background induced by Ge-68 and its effects on MDA

Fig.7 shows the background contribution of Ge-68 and its decay daughter Ga-68 in the 90 days background spectrum. As Ge-68 and its decay daughter Ga-68 are in radioactive equilibrium, we use Ge-68 to indicate Ge-68 and Ga-68 hereafter. The red line is the spectrum corresponding to $477 \mu\text{Bq/kg}$ initial activity, and the red shadow indicates the $\pm 112.4 \mu\text{Bq/kg}$ fit uncertainty. In 1-3 MeV energy region, the measured background is 90.9 ± 1.0 cpd, and the Ge-68 contributes 55.9 ± 13.2 cpd, about 62% of the measured background.

We select four characteristic γ lines from different isotopes to evaluate the effects of Ge-68 background on their minimum detection activity (MDA). The select peaks are: 583.2 keV (Tl-208), 661.7 keV (Cs-137), 1460.8 keV (K-40), and 1764.5 keV (Bi-214). The 90 days background spectrum of the four characteristic γ peaks and the contribution from Ge-68 (Ga-68) are shown in the left panel of Fig.8. For simplicity, our analysis assumes a constant background rate from the airborne radon daughter to better demonstrate the effects from the change of Ge-68 background. The improvement of MDA at different operation time in CJPL is calculated using eq.10, the results are shown in the right panel of Fig.8.

After 5 years operation at CJPL, the Ge-68 activity decreases from $477.0 \pm 112.4 \mu\text{Bq/kg}$ to $4.47 \pm 1.05 \mu\text{Bq/kg}$ and results in a 2%~8% MDA improvement for the selected four characteristic peaks. The smallest 2% improvement is for the Tl-208 583.2 keV peak as the background is dominated by Tl-208 in detector structure materials, Ge-68 only contributes 4.6% of the total background

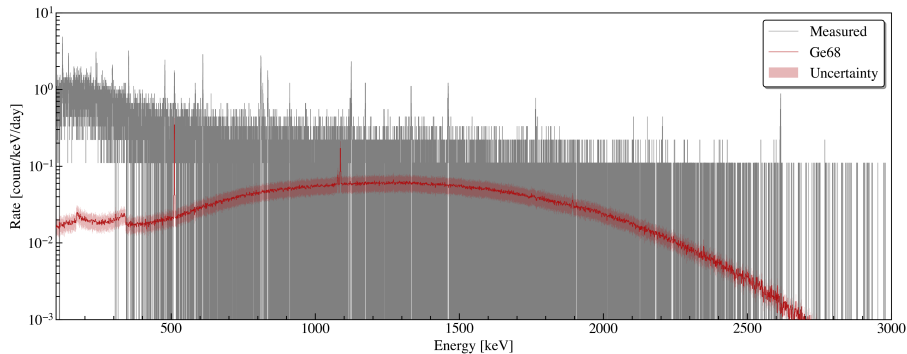


Figure 7: Comparison of measured spectrum (gray line) and simulated Ge-68 (Ga-68) spectrum (red line) with fitted activity. The fitted initial activity of Ge-68 is $477.0 \pm 112.4 \mu\text{Bq/kg}$, the red shadow is the spectra corresponding to the fit uncertainty.

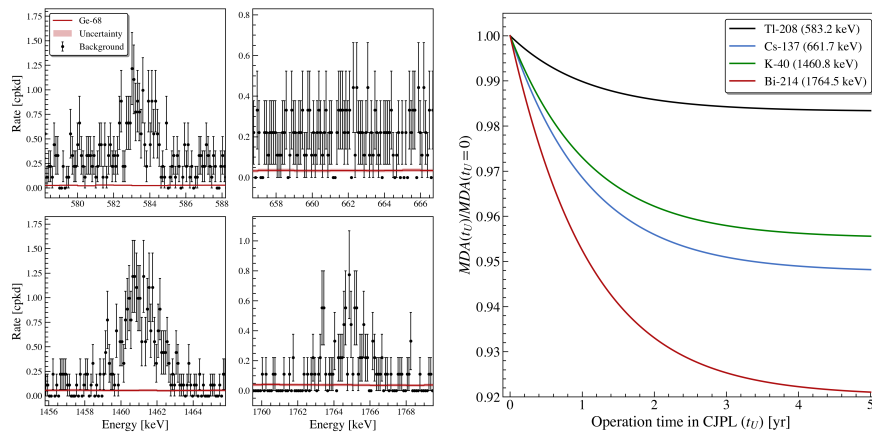


Figure 8: Left: the 90 days background spectrum in the four characteristic peak regions, contributions from Ge-68 (Ga-68) are labeled in red, the measurement of the background spectrum started about 21 days after the detector arrived CJPL. Right: the ratio of MDA between t_U and $t_U = 0$ for the four characteristic peaks.

at $t_U=0$. For the Bi-214 1764.5 keV characteristic peak, Ge-68 contributes 21% of the total background at $t_U=0$ and 0.2% at $t_U=5$ years, the about 20% background reduction gives a 8% improvement in the MDA.

3.4. Variation of airborne Bi-214 concentration

Our method also provides the concentration variation of radon daughter Bi-214 in the detector chamber. As the detector chamber within the copper shielding is constantly purged by nitrogen gas, a comparison between the variation of Bi-214 in detector chamber and radon in experiment hall indicates whether air has been mixed in the nitrogen gas or there is a leakage point in the

shielding. The radon (Rn-222) concentration in the experiment hall has been measured by an AlphaGuard PQ2000 radon monitor. The AlphaGuard is set to the diffusion mode and a measurement period of one hour. Fig.9 demonstrates the comparison of the Bi-214 and the Rn-222 concentration.

The variation of airborne Bi-214 is within 5 Bq/m^3 , its average value ($1.42 \pm 0.17 \text{ Bq/m}^3$) is about 40 times lower than the average Rn-222 concentration in experiment hall. And there is also no significant coincidence between the Bi-214 and Rn-222 concentration, indicating that the detector chamber has been well isolated from the the experiment hall.

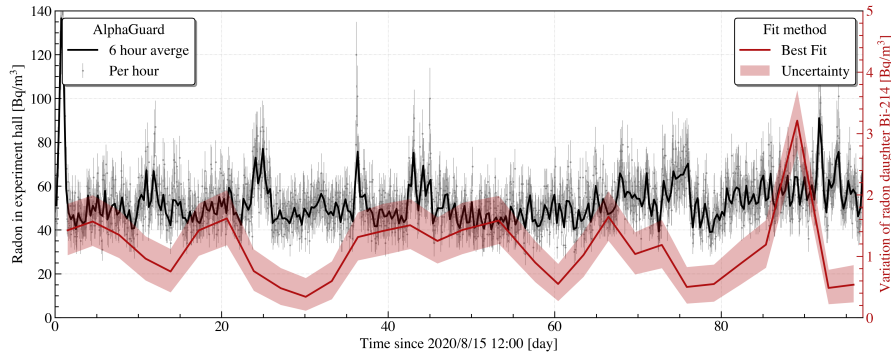


Figure 9: Variation of the radon concentration in experiment hall and the airborne Bi-214 in detector chamber within the copper shielding. The gray point and black line are the radon concentration measured by an AlphaGuard radon monitor. The red line is the fitted airborne Bi-214 concentration and the red shadow is the corresponding fit uncertainty.

4. Conclusions

In this work, we develop a time series fitting method to calculate the activity of cosmogenic Ge-68 in a coaxial HPGe detector operated at China Jinping underground laboratory. Our method using the change of count rate in 1-3 MeV energy region and characteristic peaks of airborne radon daughter to decouple the Ge-68, radon daughter, and time-invariant background and fit the Ge-68 activity. The simulated detection efficiencies in different energy region are used to connect the count rate to Ge-68 activity and airborne Bi-214 concentration. Total 90 days measured data are used in the analysis and the Ge-68 initial activity is fitted to be $477.0 \pm 112.4 \mu\text{Bq/kg}$, it contributes about 62% background in the 1-3 MeV energy region. Based on the measured background spectrum and fitted Ge-68 activity, we predict the minimum detection activity for four radioisotopes (Tl-208, Cs-137, K-40, and Bi-214) will improve by 2%~8% after 5 years underground operation.

Our method can be extended to other cosmogenic isotopes in germanium, for instance, Mn-54, Co-57, and Co-58. And the fitting result of Ge-68 activity could be used as an input in a spectrum fitting method to decouple background from different structure materials.

Acknowledgments:

This work was supported by the National Key Research and Development Program of China (Grant No. 2023YFA1607101, 2022YFA1604701) and the National Natural Science Foundation of China (Grant No. 12425507 and 12175112). We would like to thank CJPL and its staff for supporting this work. CJPL is jointly operated by Tsinghua University and Yalong River Hydropower Development Company.

References

- [1] R. D. Baertsch and N. R. Hall. IEEE Trans Nucl Sci. **17**, 3, 235-240, (1970).
- [2] W. L. Hansen. Nucl. Instrum. Methods. **94**, 377-380 (1971).
- [3] E.E. Haller. Mater Sci Semicond Process. **9**, 4, 408-422 (2006).
- [4] E. V. Bugaev, *et al.* Phys. Rev. D. **58**, 054001 (1998).
- [5] W. H. Zeng, *et al.* NUCL SCI TECH. **31**, 51 (2020).
- [6] NuDat 3.0. <https://www.nndc.bnl.gov/nudat3/>
- [7] S. Agostinelli, *et al.* Nucl. Instrum. Meth. A. **506**, 250-303 (2003).
- [8] J. Allison, *et al.* IEEE Trans. Nucl. Sci. **53**, 270-278 (2006).
- [9] J. Allison, *et al.* Nucl. Instrum. Meth. A. **835**, 186-225 (2016).
- [10] J. L. Ma, *et al.* Sci. China-Phys. Mech. Astron. **62**, 011011 (2019).
- [11] S. Turkat, *et al.* Astropart. Phys. **148**, 102816 (2023).
- [12] L. T. Yang, *et al.* Chinese Phys. C. **42**, 023002 (2018).
- [13] H. Bonet, *et al.* Eur. Phys. J. C. **83**, 195 (2023).
- [14] J. P. Chen, *et al.* Annu. Rev. Nucl. Part. Sci. **67**, 231-51 (2017).
- [15] Q. L. Zhang, *et al.* J. Tsinghua Univ (Sci Technol) (in Chinese). **64**, 1 (2024).
- [16] J. K. Chen, *et al.* (in press) (2024).
- [17] UltraNest toolkit. <https://johannesbuchner.github.io/UltraNest/readme.html>
- [18] G. Cowan. Statistical Data Analysis. Clarendon press Oxford. **4**, 46-48 (1998).
- [19] G. F. Knoll. Radiation Detection and Measurement (4th edition). Wiley (2015).
- [20] W.K.Hastings. Biometrika. **57**, 1:97-109 (1970).